Applications and evaluation of two-line atomic LIF thermometry in sooting combustion environments

2001 Meas. Sci. Technol. 12 1294

(http://iopscience.iop.org/0957-0233/12/8/342)

INSTITUTE OF PHYSICS PUBLISHING MEASUREMENT SCIENCE AND TECHNOLOGY
Meas. Sci. Technol. **12** (2001) 1294–1303 www.iop.org/Journals/mt PII: S0957-0233(01)20788-7

Applications and evaluation of two-line atomic LIF thermometry in sooting combustion environments

J Nygren[1], **J Engström**[1], **J Walewski**[1], **C F Kaminski**[2] **and M Aldén**[1]

[1] Department of Combustion Physics, Lund Institute of Technology, Box 118, S-22100 Lund, Sweden
[2] Department of Chemical Engineering, University of Cambridge, Pembroke Street, Cambridge CB2 3RA, UK

E-mail: jenny.nygren@forbrf.lth.se

Received 11 January 2001, accepted for publication 19 April 2001

Abstract
Temperature measurements using planar laser-induced fluorescence (PLIF) are most often associated with experimental challenges. In addition, no PLIF technique is generally applicable in all kinds of environment. Especially under sooting conditions problems are prone to arise, which limits the use of these techniques. In this paper the two-line atomic fluorescence (TLAF) technique was investigated in sooting environments. Indium atoms were used as thermometry species and seeded into the combustion region.

Data from two-dimensional measurements are often difficult to analyse, because of problems with treating noise. A statistical analysis method for correction of laser fluctuations was developed to increase the precision of the temperature calculations.

The results show that TLAF holds promise for temperature measurements in rich combustion, such as diesel engines, where other techniques have proven to fail. Drawbacks with the TLAF technique are that the probe volume is biased towards the post-flame zone and that seeding is required. The statistical analysis improved the precision considerably and is suitable for evaluation of other two-dimensional thermometry techniques. This paper also presents a critical review and comparison with alternatives, such as OH and NO thermometry.

Keywords: 2D-temperature, sooting environments, LIF, combustion diagnostics, statistical data analysis

1. Introduction

Measurements of temperature fields are crucial for an improved understanding of combustion processes in industrial devices. The development of improved accurate thermometry techniques for diesel engines is an especially important task, since diesel engines are becoming increasingly popular because of their highly efficient combustion in comparison to spark ignition engines. This high efficiency generally leads to lower emission of CO_2 and as a consequence diesel fuel driven engines tend to contribute less to the greenhouse effect.

Unfortunately other forms of pollution from diesel engines are still comparatively high, especially those resulting from soot and NO_x emissions. Soot particles can be reduced by higher combustion temperatures, which lead to stronger oxidation of soot particles. On the other hand, higher temperature increases thermal NO_x production. This problem highlights the importance of temperature information for the optimization of diesel engines.

In general, laser techniques are not easily applied in strongly sooting combustion environments, owing to the strong absorption, spectral interference from particulate scattering and fluorescence from large molecules. Temporally resolved temperature measurements in sooting environments are however essential for improving the overall understanding of soot formation and oxidation. A development of

novel temperature techniques for applications in sooting environment is therefore important.

Laser-based methods for temperature measurements in reactive and turbulent environments have been the subject of extensive research [1–3]. For turbulent flames, which fluctuate both in space and in time, instantaneous imaging of temperature distributions are especially desirable. The majority of such measurements have been performed in lean combustion environments and have not been optimized for applications under fuel-rich and sooting conditions.

In sooting environments, temperature measurements using line-of sight emission have recently been performed [4]. These experiments were made in order to improve the accuracy of laser induced incandescence (LII) measurements. They were used for the validation of underlying models of cooling and particularly of heat conduction in the vaporization process of soot particles. However, measurements using emission spectroscopy must be employed in a very careful manner to avoid systematic error [5]. Since emission from chemically generated species is not usually thermally equilibrated the emission method may bias temperatures to high values. These problems are discussed by Aust [6], where equilibrium temperature measurements from an SI engine are reported.

Filtered Rayleigh [7] and Raman [8, 9] scattering techniques have been used in sooting flames for both temperature and species concentration measurements. These techniques revealed reliable information in sooting environments, but the accuracy is limited since knowledge of the collisional cross-sections is required for all involved species [10]. This would tend to limit these techniques for thermometry applications in practical environments with non-homogeneously mixed systems, such as diesel engines, where local effective cross sections are unknown. Furthermore, in realistic engine geometry strong elastic scattering from surfaces may also cause problem.

A thermometry technique that is applicable in sooting environments is coherent anti-Stokes Raman spectroscopy (CARS). This is a technique used for point-wise measurements of temperature and major species concentrations, which is described in [11–14].

Different thermometry applications based on laser-induced fluorescence (LIF) techniques have been reviewed by Daily [15]. In the simplest approach of LIF, the temperature is deduced from the intensity of a single transition. For such measurements to be precise, however, the variation of mole fraction and collisional quenching in the reacting flow must be accounted for quantitatively. In highly sooting and turbulent flames this task is almost impossible. These problems can be avoided by extracting the temperature from the ratio of two LIF signals from two temperature transitions and determining a two-line Boltzmann temperature [16]. A disadvantage of two-line LIF methods is that they are experimentally complex, since two laser and gated detector systems are required. A quantitative comparison of the two approaches is found in [17].

LIF thermometry can be based either on seeded species or on native molecules in the combustion process. One of the most commonly used species is the OH radical [3, 18, 19], which, however, exhibits low concentrations in fuel-rich and sooting flames due to the low prevailing temperatures and low levels of oxidizing species present [20]. For applications of LIF thermometry in such flames, the use of seeded species may be a preferable choice [10]. However, when tracer species are seeded into the combustion process, it is essential that their influence on the combustion process is negligible.

Recently, Bessler *et al* have shown temperature distributions in rich flames based on two-line thermometry of seeded NO [21]. The characteristics of NO molecules as flame temperature markers have been discussed in detail in [17], showing that one advantage of this approach is that it provides information about the temperature, in both pre- and post-flame zones. Since NO is a chemically active combustion species significant reduction effects of seeded NO concentrations have been observed in flames [22]. This reduction is produced by a combination of reburn chemistry and dilution. The reburning of NO has the largest influence in rich flames where NO reacts with CH producing HCN and O. This reaction will in turn increase the oxidation of soot particles since more oxygen becomes available. The effects are exacerbated by the fact that large amounts of NO are required to achieve the signal to noise ratios required for LIF thermometry. Thus careful checks have to be carried out to control that seeded NO does not interfere with the combustion process. Furthermore, when molecular species are employed for thermometry, corrections for rotational and vibrational energy transfer processes have to be performed [23].

In the latter respect, a temperature evaluation from atomic species is far easier according to the simpler spectroscopic features of an atom [15]. Thermometry measurements have been performed with thermally assisted fluorescence (THAF) in fuel-rich flames using seeded gallium atoms [24]. A disadvantage with this technique is that knowledge of collisional cross-sections for all involved species is required. Further, due to low signal levels THAF does not seem to be applicable for temperature measurements in engines on single shot basis. Two-line atomic fluorescence (TLAF), on the other hand, has recently been reported to provide this [25]. TLAF is based on suitable atoms being seeded into the combustion region and indium has been pointed out to be an attractive candidate for practical combustion, since it is sensitive over a wide temperature range (700–3000 K) [26]. It has also been shown that indium TLAF holds promise for temperature measurements in highly sooting flames [27]. It has been shown that the number density of TLAF active indium atoms increases in fuel-rich flames, with the result that very low seeding concentrations can be used. However, a limitation of the technique is that only regions behind the flame front are accessible by the technique, owing to the process by which indium is produced in flames.

The purpose of this paper is twofold. The first part is experimental, where a two-dimensional approach for TLAF in highly sooting flames has been performed. The fluorescence signals were measured and the temperature was evaluated for different equivalence ratios (Φ) in an atmospheric acetylene/air flame. Furthermore we simultaneously measured the profiles of indium and OH LIF signals as a function of flame stoichiometry. The results indicate the preferred flame region in which to perform LIF thermometry approaches on indium or on OH. In particular it is shown that the OH thermometry is towards high temperature regions and difficult to apply in sooting environments.

Since adding metallic ions may change the soot production [28], laser induced incandescence (LII) measurements were

conducted for different seeding concentrations to see whether the indium atoms affected the flame chemistry. Absorption measurements were also performed on a diesel flame, to investigate the applicability of TLAF to diesel combustion.

In the other part guidelines of how two-dimensional data is analysed in the best possible way is presented. In contrast to earlier studies [27, 29], we recorded in the present work both the TLAF signals and the laser intensity profiles on a shot by shot basis. In this way a correlation between the two can be calculated. By accounting for this correlation the statistical error of the measured temperature can be reduced substantially. Furthermore, the upper precision limit of TLAF in a sooting environment can be stated in this way. Although this analysis was performed in the particular context of TLAF, the results are general and applicable to other thermometry techniques as well.

2. Theory background for TLAF

The theory of TLAF is described in detail in [15] and references therein. Briefly, suitable metal atoms [26], having two optically accessible and temperature-sensitive energy states 0 and 1, are seeded into the combustion environment. The absorption wavelengths of these transitions are λ_{02} and λ_{12}, respectively. Two time-delayed laser pulses with the corresponding wavelengths are then used to excite the two states to a common upper state 2. The corresponding LIF signals, F_{20} and F_{21}, are collected by two detectors equipped with interference filter. In thermal equilibrium the ratio F_{21}/F_{20} is proportional to the Boltzmann factor containing the temperature T of the system. It can be shown that the temperature is given by

$$T = \frac{\Delta E/k_B}{4\ln(\lambda_{21}/\lambda_{20}) + \ln(F_{20}/I_{12}) - \ln(F_{21}/I_{02}) + \ln C} \quad (1)$$

where ΔE is the energy difference between the two lower states involved, k_B is the Boltzmann constant and I_{i2} ($i = 0, 1$) are the laser intensities. C is a system-dependent calibration constant that needs to be determined separately and includes factors such as spectral overlap between laser and atomic line-widths, detector and light collection efficiencies etc. The effects of quenching cancel out in the expression for T, since the excitation for each fluorescence process is to the same upper state, and therefore the quenching is exactly the same. Equation (1) is valid under the assumption of a linear relationship between laser intensity and LIF signal. Therefore, effects of saturation and self-absorption must be carefully checked for in a given measurement situation. Self-absorption tests are especially important in fuel-rich flames where the number of absorbing atoms may increase because of the lower oxidation rate of free atoms [27].

LIF in sooting hydrocarbon flames can suffer from a large amount of signal background which arises from laser produced C_2 [8], LIF of PAH:s and LII from soot particles. Corrections for these interference are of major importance to obtain accurate results. In TLAF applications with indium, no such interfering effects were found in rich flames [27]. The reason for this is the low laser intensities required for TLAF, which reduce the LII from soot particles.

Furthermore, extinction of both laser radiation and emitted fluorescence from soot particles and hydrocarbons will also appear in sooting flames. In general longer excitation wavelengths should be used since absorption by soot particles scales as the inverse of the wavelength. For TLAF application this mean that trapping effects are different for the two excitation wavelengths. Trapping effects result in lower signal and decreasing accuracy of the measurement, since the laser energy at the measurement location needs to be known. This results in an unknown inaccuracy on the evaluated temperature. The best strategy is to make linearity checks to avoid trapping effects, both for laser attenuation and for the self-absorption.

3. Experimental methods

3.1. Temperature measurements

The experiments were performed in a slot burner ($100 \times 1\ \mathrm{mm}^2$) fitted with a standard analytical flame atomizer assembly (Perkin Elmer). The flame was an atmospheric pressure acetylene (C_2H_2)/air flame seeded with aqueous solutions of indium chloride ($InCl_3$). Investigations were carried out for various stoichiometries (Φ) rising from $\Phi = 1.0$ to 3.5. This value was varied by increasing the C_2H_2 flow, which means that the overall mass flows and the corresponding flame profiles were changing during measurements. The flame flows were maintained by mass-flow controllers and the flame was assumed to be reproducible during the experiments by adjusting the mass-flow controllers to the same values again. Only the stoichiometric flame was free from soot particles.

The excitation wavelengths at 410 nm and 451 nm were obtained from a Nd:YAG-pumped optical parametric oscillator (OPO, Spectra Physics MOPO 730-10) with a frequency doubler providing radiation, corresponding to the $5P_{1/2} \rightarrow 6S$ and $5P_{3/2} \rightarrow 6S$ transition of indium. The experimental set-up is shown in figure 1.

A waveplate/polarizer assembly was used to allow precise control of the laser intensities and to ensure excitation in the linear regime. TLAF signals were found to be linear up to 20 μJ/pulse, approximately corresponding to a spectral energy density of $3 \pm 1 \times 10^3\ \mathrm{W\,cm^{-2}\,cm^{-1}}$ in the measured area. The beam was formed into a sheet ($20 \times 0.3\ \mathrm{mm}^2$) by a cylindrical telescope and a slit, and passed through the flame at 7 mm above the burner head.

Using an intensified CCD camera (LaVision Flamestar II, 384×576 pixels) arranged perpendicular to the incoming laser sheet fluorescence signals were detected. The burner was placed so that the fluorescence signal had a pathway of approximately 85 mm through the flame. The camera was equipped with a standard 50 mm lens (Nikon) and an interference filter with a peak transmittance at either 410 nm (F_{20}) or 451 nm (F_{21}) and a FWHM of 10 nm. Laser beam profiles were monitored on-line by simultaneously imaging the fluorescence from a water solution containing fluorescing dye. The purpose of this was to account for signal fluctuations caused by the laser source (see section 4.5). During the measurement the laser was tuned to reach the two indium-TLAF transitions, and the fluorescence from each transition was measured. With this arrangement only average temperatures could be evaluated which is adequate for laminar flames.

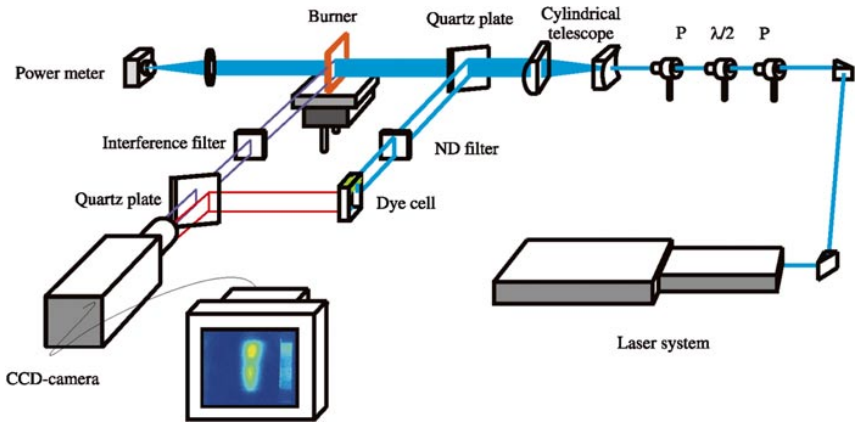

Figure 1. Experimental set-up for the two-dimensional TLAF measurement. A quartz plate was used to reflect a few per cent of the laser to perform on-line beam profile measurements.

For turbulent flows, F_{20} and F_{21} have to be measured on a time scale which is shorter than turbulence time scales, which in practice means that two lasers and two detectors have to be used simultaneously as described in [29].

3.2. Simultaneous indium/OH LIF measurements

The deviation of the fluorescence profiles from OH and indium was investigated, both in the slot burner and in small pool-flames in a cup burner with different liquid fuels. Since the latter fluctuated in time, OH and indium measurements had to be performed simultaneously and two laser and detector systems were used. The slot-burner was operated under identical conditions as described in section 3.1. The cup burner had a diameter of 30 mm. Methanol, diesel and JET-A were examined.

In addition to the OPO (see section 3.1) a standard Nd: YAG / dye system (Continuum) was used for OH excitation. For the OH measurements, the Q_1 (8) line in the $X\,^2\Pi(v = 0) \rightarrow A\,^2\Sigma(v = 1)$ band at $\lambda = 283.68$ nm was excited using a pulse energy of approximately 6×10^7 W cm^{-2} cm^{-1}. This excitation line was chosen because its population is the least temperature sensitive (varying by less than 5% between 1400 and 2100 K [1]). The two laser beams were combined using a specially coated quartz plate, formed into sheets and carefully aligned through the flame to ensure excitation in same region as those in which the temperature measurements were previously performed. Two filtered intensified CCD cameras, arranged at right angles to each other and aligned on a pixel by pixel basis, monitored the fluorescence signals, at 309 nm for OH and at 410 nm for indium. The filter in front of the camera that monitored the OH signal was an interference filter with a peak transmittance of around 312 nm and a FWHM of 20 nm. A beam splitter was used to separate the two fluorescence signals. A similar experimental set-up can be seen in [25].

Background images were recorded for all the LIF measurements by tuning the laser slightly off the resonance frequency for respectively species. The background images were then subtracted from the fluorescence signals in order to eliminate contributions to the signal from soot and PAH. When the laser was tuned off for the OH excitation line, the fluorescence signal from the OH-molecules disappeared, but scattered light from soot particles and LIF from PAH could still be observed. However, since the off-resonance profile was obtained just by changing the laser wavelength by 0.1 nm, no differences in signal strength could be detected, either for the scattered light from the soot particles or for the PAH fluorescence, when identical laser energies were used. Thus, the pure OH fluorescence signal could be obtained, even in the presence of soot particles, when the off-resonance image was subtracted from the resonance image. No corrections for laser attenuation (<3%), temperature or trapping effects was made. In contrast to the OH imaging, hardly any laser-induced background was detected in the TLAF experiments, even in the most sooting flame.

3.3. Laser-induced incandescence measurements

It has been discussed in the literature [30] that adding metallic complexes may either decrease soot formation or increase the rate of soot oxidation. There are different mechanisms that affect the soot formation of the seeded metal and it is almost exclusively dependent on temperature, seeding concentration and ionization potential [28]. One mechanism is that metal ions are expected to increase the nucleation rate and lead to smaller individual particles for a given carbon yield and therefore to higher chemical rate oxidation. Therefore LII was used to measure the soot volume fraction and the soot particle size as a function of seeded indium concentration. The measurements were performed in the region 7–22 mm above the burner head. In this experiment the slot burner was arranged so the camera was placed perpendicular to the slit. Two flames with different equivalence ratios $\Phi = 2.5$ and 3.5 were investigated and both the soot volume fraction and the size of the soot particles were measured. Each flame measurements were performed with two different seeding solutions, one with a solution of indium and distilled water and the other with only distilled water. Details of the LII technique are found in [31, 32].

3.4. Spectroscopic studies

Feasibility spectroscopic studies were also carried out in the cup burner flame for these fuels. First, experiments were made using a xenon lamp to establish the expected laser beam attenuation from absorption and extinction for different wavelengths. Secondly, experiments were made to investigate

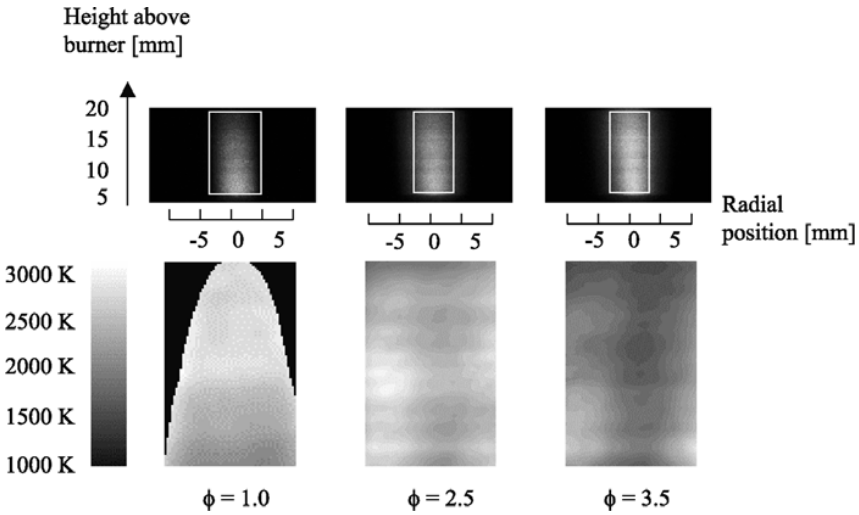

Figure 2. The upper row shows fluorescence images from the excitation at 410 nm. The bottom row shows the resulting images obtained from two-dimensional TLAF. The images correspond to three Φ-values, 1.0, 2.5 and 3.5 from the marked region above. Black regions correspond to pixels with a too low SNR for temperatures to be evaluated.

whether other species in the flames were interfering with the detected TLAF signals. Here the laser was scanned across the absorption lines for indium and the fluorescence was focused onto the entrance slit of a spectrograph (SpectraPro-150 monochromator) using an $f = 100$ mm lens. The emission light was spectrally resolved using a grating of 1200 grooves mm^{-1} and detected by the ICCD camera.

4. Result and discussion

4.1. Temperature measurements

Figure 2 shows temperature distributions obtained from the slot burner for $\Phi = 1.0$, 2.5 and 3.5. These images correspond to temperatures evaluated from an average of 50 single-shot images for each fluorescence signal. For each individual fluorescence image, an average background was subtracted and the image corrected by the corresponding laser profile as described in equation (1). Only pixels with signals larger than 40 counts were used in the evaluation of the temperature. This signal-to-noise (SNR) criterion was chosen to obtain a sufficient precision of the evaluated temperature. This is described in more detail in section 4.5. Only temperatures higher than 700 K are displayed in the images, corresponding roughly to the lowest temperature where indium TLAF becomes sensitive [25]. All other pixels were ignored in the calculations, i.e. black areas in the images correspond to pixels where the SNR or the calculated temperatures were too low for evaluation of temperatures.

Calibration measurements of the flame temperatures were conducted using coherent anti-Stokes Raman spectroscopy (CARS). A variant called dual broadband rotational CARS [33, 34] was used for these calibration measurements.

In figure 2 the features of the flame temperature distribution are shown and they are in agreement with other measurements [35, 36]. The highest temperature was obtained for $\Phi = 1$, with a peak value of around 2400 K, roughly 200 K lower than the adiabatic flame temperature, most probably due to heat losses to the burner and the presence of seeded water. For $\Phi = 1$ the flame was a well defined premixed laminar flame and, as seen in the image, the temperature increased with height above the burner head.

For increasing Φ-values, a significant change of the flame shape was observed. In the more fuel-rich flame, the mass flow increased and the burning velocity of the mixture became lower. As a result the flame size became larger, and the reaction zone shifted up and to the outer part of the flame. As the soot concentration increased, both the OH concentration and the flame temperature are found to decrease. The characteristic of these fuel-rich flames is better described as diffusion flames than as premixed flames. The detected temperatures were lowest for the most sooting flame according to effects in the flame chemistry [37], heat radiation from the soot particles and the fact that the location of the measurement was kept fixed while the flame shape changed with increasing Φ-value.

4.2. Simultaneous measurements of OH and indium fluorescence

In figure 3 simultaneous images of OH and indium fluorescence are shown. As seen in this figure there was a significant difference in the detected fluorescence profiles of OH and indium. The changes of the reaction zone and the different flame size can also be observed in the figure. Note that the grey scale in the images reflects relative LIF intensities and only approximately reflects relative concentrations of imaged species. The OH distributions reflect both regions of high temperatures and the position and shape of reaction zones. Towards lower temperatures (below ∼1200 K) [38], OH is rapidly consumed and below detection limit of LIF. In the fuel-rich and sooting flames the concentration profiles are symmetrically placed around the burner centreline.

Figure 4 represents the signal profiles of OH, indium and soot/PAH. From this figure one can see a distinct feature arising from OH fluorescence in the primary reaction zones (the outer part of the flame) and scattered light from soot particles and PAH fluorescence in the rich flame regions (closest to the

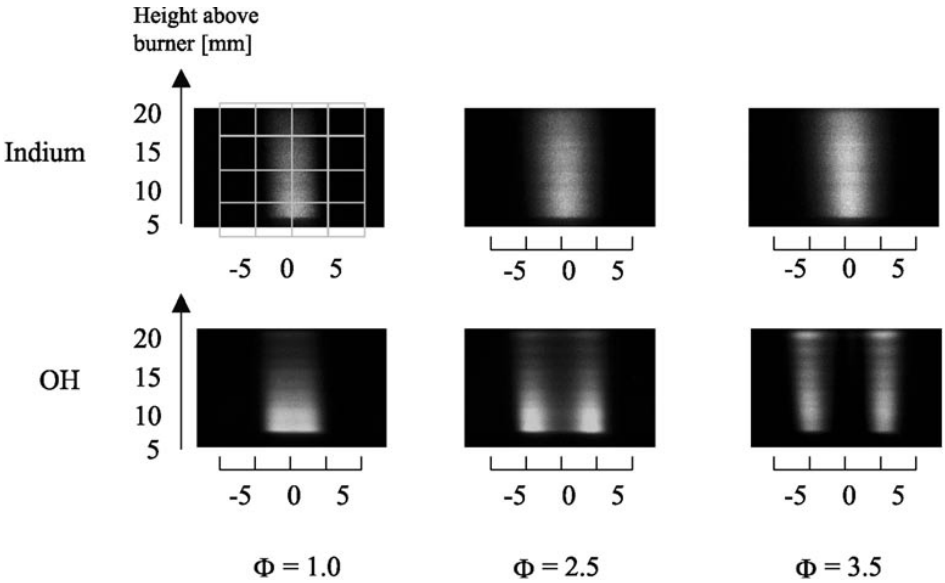

Figure 3. Simultaneous fluorescence images of indium and OH in flames for $\Phi = 1.0$, 2.5 and 3.5. Note the differences between the distributions for the fuel-rich cases. The x-axis shows the radial position in mm.

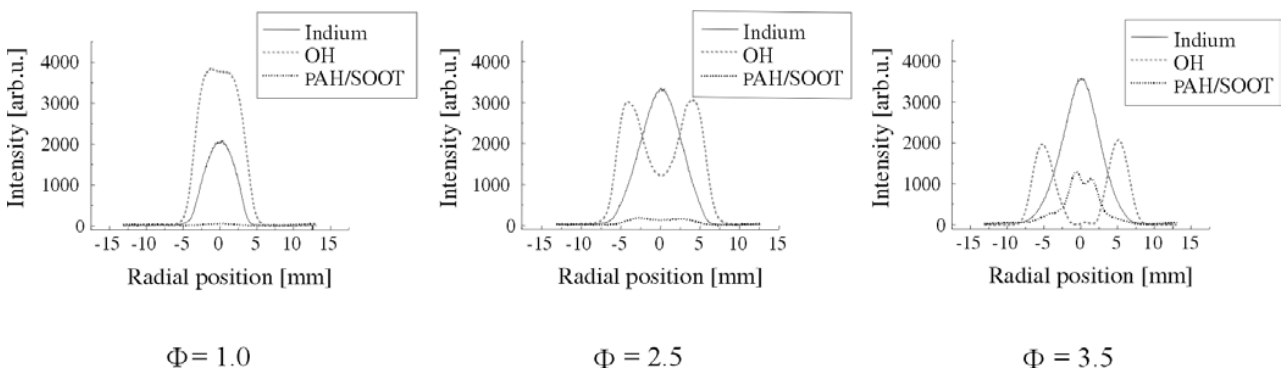

Figure 4. Concentration profiles through the flame in which the variation of the fluorescence intensities for OH, indium and the PAH/soot is clearly seen for $\Phi = 1.0$, 2.5 and 3.5. The measurement region was 7–22 mm above the burner.

central line). No OH was detected near the centreline, where soot and PAH were concentrated, since soot oxidation reduces the amount of OH radicals, which is a reactive partner in a three-body recombination reaction [20].

From figure 3 it is clear that TLAF signals are substantial only in the core region of the flame where OH concentrations are low. Previous experiment have indicated that oxidation may play a major role in the production of TLAF active neutral indium [27]. In fuel-rich zones, where less oxygen is available, the atomization process becomes more efficient and corresponding stronger TLAF signals are obtained. On the other hand, in areas where the concentration of OH or oxygen is large the result is loss of TLAF signal. This is clearly shown in figure 4, obtained from the measurement images.

In the flame with $\Phi = 1$, the OH and the indium profile gradients are similar, in contrast to highly sooting flames or diffusions flames, where a distinct shift in the gradient was detected between the two species. As can be seen in the diagram for higher Φ-values, the TLAF signals were detected with a decreasing intensity towards the OH signal. This suggests that, depending on the flame characteristic, the production zones of OH and seeded atoms will have more or less of an overlap.

This deviation in LIF profiles for OH and seeded atoms will effect the measured temperature information. In premixed flames with $\Phi \approx 1$, the detected area is almost the same and a similar evaluated temperature is expected. In diffusion flames, completely different temperature distribution images will be found. For example, in highly sooting areas no temperature information will be conducted with OH thermometry. Therefore the evaluated temperatures are expected to reveal that the OH thermometry is towards the high temperature regions, where most OH-radicals are produced [25, 36]. Furthermore, in lean combustion where a lot of OH and O_2 are present the fluorescence signal from the indium atoms will not be sufficiently high to yield temperature information if the seeding concentration is not increased. Before the seeding concentration is increased a careful control has to be done to investigate that no effects on the combustion occurred. In lean combustion devices the higher seeding concentration required may cause practical limitation by window deposit of indium oxide [39].

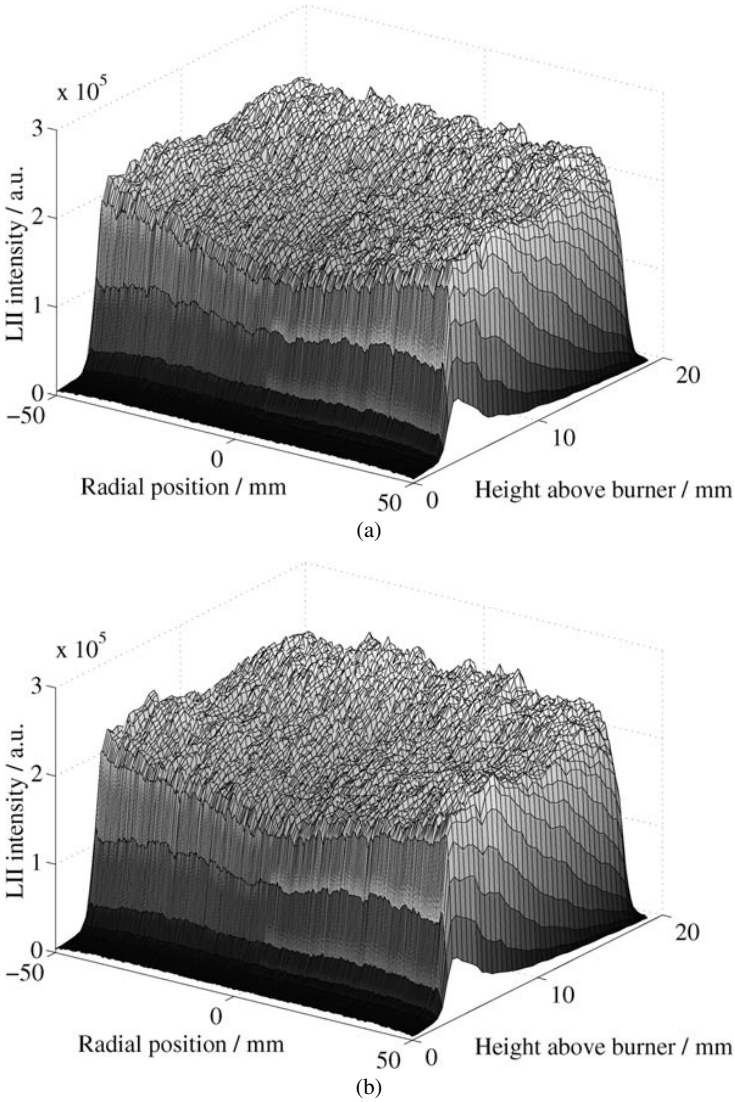

Figure 5. The distribution of the soot volume fraction for $\phi = 3.4$ and different seeding solutions: (a) 500 mg l^{-1} of $InCl_3$, (b) distilled water.

4.3. Laser-induced incandescence measurements

The resulting images from the LII measurements, which were performed in order to control whether indium affected the combustion, can be seen in figures 5(a) and 5(b). The distribution of the soot particles in the flame can be observed in those images where the soot volume fraction is presented. The x-axis shows the position in the flame, the y-axis the soot volume fraction. From the z-axis the height above the burner head can be seen. The results from these LII measurements show that, within the accuracy (around 30%) of the technique [40], neither differences in the particle size nor differences in the soot volume fraction could be observed for different $InCl_3$ seeding solutions, 100–1000 mg l^{-1}. The result presented in figure 5 show one solution with an $InCl_3$ concentration of 500 mg l^{-1} and one with distilled water. If the indium atoms had influenced the combustion process and the chemical reactions, a change should have been seen in the soot volume fraction between the different seeding solutions, with and without indium, and on the particle sizes. The possible influence on the soot volume fraction caused by the water is not a problem, since in more practical applications, such as engines and turbines, the indium can be directly dissolved in the fuel and no water needs to be added [25, 29, 39].

4.4. Spectroscopic studies

The absorption measurements in the cup burner flame showed that no signal contribution caused by interfering species could be observed, for the excitation wavelengths of indium, when diesel was used as fuel. No differences in the absorption were observed between the used wavelengths. This seems promising for future applications where diesel is used as fuel.

Other difficulties that might occur in an application in a diesel engine are decreasing window transparency as a result of soot deposition. The amount of deposit soot will change during the measurement and therefore also the laser beam passing through the engine. This fact will cause a problem when the fluctuation of the laser beam should be taken into account, which is discussed in section 4.5, since the in-cylinder attenuation of the laser sheet intensity also needs to be accounted for in this case. Strategies and image processing are discussed in [41, 42]. This problem is general for all

optical techniques and will limit the accuracy of the evaluated parameter.

4.5. Data analysis

In a 2D application it is important to make corrections for the spatial laser intensity distribution to obtain reliable and correct information from the LIF images. It is equally important to investigate the impact of laser intensity fluctuations on the LIF signals. Both should preferably be recorded on a shot-to-shot basis. In this section a statistical treatment and discussion will be presented to put this on a quantitative footing. Similar investigations have been reported by Seitzmann *et al* [43], showing the importance of these corrections. The measurements were analysed with respect to the statistical uncertainty of evaluated temperature, which is introduced by laser intensity fluctuations. The precision of a technique is defined as the variability of the measured parameter due to noise and/or random measurement variations. The associated measurement errors in equation (1) result from an additive combination of errors from F_{20} and F_{21} and the laser intensities I_{02} and I_{12}. This is the way in which the error analysis was treated in earlier publications [27, 29]. In this work TLAF signals and laser intensities were measured simultaneously, providing a measure for the correlation of signal and laser fluctuations. This allows us to eliminate the contribution of laser intensity fluctuations to the uncertainty of the calculated temperature. The expression for the statistical error and a more detailed discussion can be found in the appendix.

A discussion on errors associated with 2D TLAF is found in [29]. The reported precision of evaluated temperatures was 14%, a figure suggested to improve by on-line intensity profile measurements of the laser source. All errors stated here are σ_T/T. Taking laser fluctuations into account the statistical error of the temperature was found to decrease by 20–50% in this work. The value depends on the signal strength. This means that at least 20% of the statistical error of the temperature is caused by laser fluctuations, which can be easily corrected for. For the presented data a precision of at best 8–9% for a single CCD pixel was obtained when corrections for laser fluctuations were made. This value only contains contributions from detector noise and flame fluctuations and presents an upper precision limit for TLAF measurements in this work. One can reduce the detector noise error by averaging pixels with their neighbours (thereby reducing spatial information). The precision will then improve by a factor of the square root of the number of pixels. Averaging pixels, 2×2 or 3×3, improving the precision to 3–4% for the present data, which is a value of the same order as reported by Dec and Keller [44] for point measurements in turbulent flames.

In any case, it is not always possible to measure the laser intensity profiles on a shot-to-shot basis. In this case the precision can be substantially improved by using more stable laser sources. Our laser system showed laser fluctuations $\sigma_I/I \approx 5$ and 10% for 451 and 410 nm, respectively. Suggesting available lasers with stability $\sigma_I/I < 2\%$ on the respective excitation wavelength it is possible to reach the same precision as in this work without correcting for laser fluctuations. The value of the statistical uncertainty itself is overall depending on the stability of the flame.

Indium-TLAF is also favourable in statistical terms compared with OH-thermometry in fuel-rich and sooting flames, since the S/N yields for indium-TLAF signals are much higher due to the reductive processes of OH in such environments. Higher signal levels increase the precision of the evaluated temperature.

5. Conclusion

Two-line atomic fluorescence was demonstrated for two-dimensional temperature measurements in highly sooting environments. The experiments were performed in a slot-burner with stoichiometries varying between 1.0 and 3.5. LII measurements were carried out to investigate whether the seeded indium atoms caused any effect on the flame chemistry. Within the uncertainty limit of the LII technique, no influence on the soot volume fraction could be observed for different amount of indium seeded into the flame.

We showed that laser fluctuations can lead to a significant bias in the precision of evaluated temperatures. These are not corrected for by standard error analysis methods, which are commonly used in this context. The presented treatment of the data can improve the precision of the technique within 20–50% for a sufficient S/N ratio if compensation is made for laser fluctuations. This improvement can be made if an online beam profile is measured for each single-shot fluorescence image. This analysis is not restricted to the current method but is applicable to all ratiometric measurement techniques.

These measurements show promising results for using the TLAF technique in future two-dimensional temperature applications in diesel engines, since the technique did not appear to be disturbed by soot particles and no detectable attenuation of the laser was seen in diesel combustion. From the spectroscopic studies of the absorption from different fuels, only a small absorption was observed for the used indium wavelengths 410 and 451 nm.

Simultaneous indium and OH fluorescence images were measured for different stoichiometries. The results from these investigations showed that the regions where the species were measured changed with increasing Φ-values. These simultaneous recorded In/OH images indicate that when using OH thermometry the measured region is biased towards the high temperature side and when using temperatures obtained with indium TLAF, the temperature information originates from more fuel-rich and hence colder parts.

Acknowledgments

We gratefully acknowledge the financial support by the Swedish National Energy Administration, the Swedish Research Council for Engineering Science and the Centre of Competence: Combustion Processes.

The authors also thank Boman Axelsson and Robert Collin for the LII measurements, Joakim Bood and Christian Brackmann for the CARS measurements and Thomas Metz for fruitful discussions about statistical data analysis.

Appendix

The statistical investigations include an analysis of different experimental sources of uncertainty and their influence on the precision of TLAF. The main aim of the investigation is to improve the precision of the evaluated temperature and to give an upper limit for the precision of the temperature. The questions analysed here are the statistical uncertainty of evaluated temperatures from different types of source like laser fluctuations and detector noise. The measurement errors of the temperature evaluated from TLAF when only accounting for linear correction terms can easily be derived from equation (1) [45, 46].

$$\left(\frac{\sigma_T}{T}\right)^2 = \left(\frac{kT}{\Delta E}\right)^2\left[\left(\frac{\sigma_{F_{21}}}{F_{21}}\right)^2 - 2\frac{\mathrm{cov}(F_{21}, I_{02})}{F_{21}I_{02}} + \left(\frac{\sigma_{I_{02}}}{I_{02}}\right)^2 + \left(\frac{\sigma_{F_{20}}}{F_{20}}\right)^2 - 2\frac{\mathrm{cov}(F_{20}, I_{12})}{F_{20}I_{12}} + \left(\frac{\sigma_{I_{12}}}{I_{12}}\right)^2 + \left(\frac{4\sigma_{\lambda_{21}}}{I\lambda_{21}}\right)^2 + \left(\frac{4\sigma_{\lambda_{20}}}{I\lambda_{20}}\right)^2 + \left(\frac{\sigma_C}{C}\right)^2\right] \quad \text{(A1)}$$

where σ_x/x denotes the relative error in the quantity x and $\mathrm{cov}(x, y)$ the covariance of the quantities x and y. The relative uncertainty of the excitation wavelength is substantially lower than that of the variables [47] and therefore $\sigma_{\lambda_{21}} = \sigma_{\lambda_{20}} = 0$. σ_C/C is within 2% according to the accuracy of CARS. Here it is assumed that the laser source has a much broader bandwidth than the absorption lines. Therefore the uncertainty of the line overlap is assumed to be zero.

Similar expressions for the uncertainty of the temperature in earlier publications [27, 29] did not contain the covariance terms in equation (A1). Laser fluctuations were suggested to have a pronounced influence on the uncertainty of the evaluated temperature. Indeed, when taking these fluctuations into account according to equation (A1), σ_T was found to decrease between 20 and 50% in this work. The value depends on the signal intensity. Figure A1 shows an example of the difference in the standard deviation of the temperature T with and without covariance terms in equation (A1).

Due to a read-out error for one of the excitation wavelengths, a rectangular gap appeared both in the laser and the LIF profile in the region: height = 10.2–13.8 mm. This introduces an uncertainty on the laser intensity and the LIF signal. Anyhow, both signals were distorted at the same time, which entails a strong correlation between them. When correcting for this correlation, by calculating the covariance terms in equation (A1), the uncertainty due to the read-out error vanishes.

As seen in equation (A1) the precision of the determined temperature increases with increasing separation between the two lower energy levels. The accuracy of the temperature measurements depends on the temperature sensitivity, which is a function of the energy spacing between these two levels and their relative population at different temperatures. Furthermore, when the relative statistical errors of the measured variables are fixed, the relative error of the evaluated temperature is inverse proportional to the temperature itself. This is similar for other two-line thermometry methods. This means that the relative precision of the measured temperature benefits from lower temperatures. However, the anti-Stokes fluorescence signal F_{20} decreases with increasing ΔE and increase with higher temperature. In practice care has to be taken so that the SNR is maximized in combination with an acceptable precision. It has been suggested [3, 15] that good temperature sensitivity in general is obtained if $\Delta E/k$ is comparable to the maximum temperature of interest.

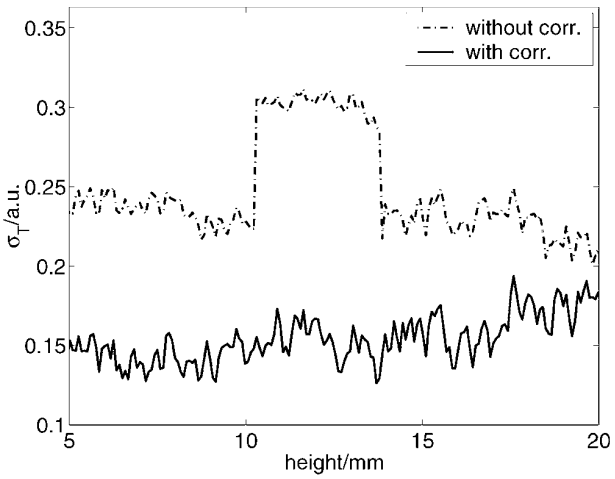

Figure A1. This figure shows an example of the difference in the standard deviation of the temperature T with and without covariance terms in equation (A1) ($\Phi = 2$). Notice the strong deviations of both curves between 10 and 15 mm height, which are due to read-out error in one of the In LIF images.

References

[1] Eckbreth A C 1996 *Laser Diagnostics for Combustion Temperature and Species* 2nd edn (Amsterdam: Gordon and Breach)

[2] Laurendeau N M 1988 Temperature measurements by light-scattering methods *Prog. Energy Combust. Sci.* **14** 147–70

[3] Kohse-Höinghause K 1994 Laser techniques for the quantitative detection of reactive intermediates in combustion systems *Prog. Energy Combust. Sci.* **20** 203–79

[4] Schraml S, Dankers S, Bader K, Will S and Leipertz A 2000 Soot temperature measurements and implications for time-resolved laser induced incandescence (TIRE-LII) *Combust. Flame* **120** 439–50

[5] De Iuliis S, Barbini M, Benecchi S, Cignoli F and Zizak G 1998 Determination of the soot volume fraction in an ethylene diffusion flame by multiwavelength analysis of soot radiation *Combust. Flame* **115** 253–61

[6] Aust V, Zimmermann G, Manz P-W and Hentschel W 1999 Crank-angle resolved temperature in SI engines measured by emission-absorption spectroscopy *SAE Paper* 1999-01-3542

[7] Hofmann D and Leipertz A 1997 Temperature field measurements in a sooting flame by filtered Rayleigh scattering (FRS) *Proc. Comb. Inst.* **26** 945

[8] Brockhinke A, Hartlieb A T, Kohse-Höinghaus K and Crosley D R 1998 Tunable KrF laser-induced fluorescence of C_2 in a sooting flame *Appl. Phys.* B **67** 659

[9] Rabenstein F and Leipertz A 1998 One-dimensional, time-resolved Raman measurements in a sooting flame made with 355 nm excitation *Appl. Opt.* **37** 4937

[10] Hartlieb A T, Atakan B and Kohse-Höinghaus K 2000 Temperature measurements in fuel-rich non-sooting low-pressure hydrocarbon flames *Appl. Phys.* B **70** 435

[11] Greenhalgh D A 1988 *Advances in Non-linear Spectroscopy* (New York: Wiley) pp 193–250

[12] Stricker W and Meier W 1993 The use of CARS for temperature measurements in practical flames *Trends Appl. Spectrosc.* **1** 231
[13] Bengtsson P-E, Martinsson L, Aldén M and Kröll S 1992 Rotational CARS thermometry in sooting flames *Combust. Sci. Technol.* **81** 129–40
[14] Bengtsson P-E, Aldén M, Kröll S and Nilsson D 1990 Vibrational CARS thermometry in sooty flames: quantitative evaluation of C_2 absorption interference *Combust. Flame* **82** 199–210
[15] Daily J W 1997 Laser induced fluorescence spectroscopy in flames *Prog. Energy Combust. Sci.* **23** 133–99
[16] Zizak G, Omenetto N and Winefornerr J D 1984 Laser-excited atomic fluorescence techniques for temperature measurements in flames: a summary *Opt. Eng.* **23** 749–55
[17] Tamura M, Luque J, Harrington J E, Berg P A, Smith G P, Jeffries J B and Crosley D R 1998 Laser-induced fluorescence of seeded nitric oxide as a flame thermometer *Appl. Phys.* B **66** 503
[18] Cattolica R 1981 OH rotational temperature from two-line laser-excited fluorescence *Appl. Opt.* **20** 1156
[19] Meier U M, Wolff-Gaßmann D, Heinze J, Frodermann M, Magnusson I and Josefsson G 1999 LIF imaging of species and temperature in technical combustion at elevated pressures *18th Int. Congr. on Instrumentation in Aerospace Simulation Facilities (Toulouse, 1999)*
[20] Haudiquert M, Cessou A, Stepowski D and Coppalle A 1997 OH and soot concentration measurements in a high-temperature laminar diffusion flame *Combust. Flame* **111** 338–49
[21] Bessler W, Hildenbrand F and Schultz C 2000 Vibrational temperature imaging using two-line laser-induced fluorescence of seeded NO *Laser Applications to Chemical and Environmental Analysis, Tech. Digest, (Santa Fe, 2000)*
[22] Atakan B and Hartlieb A T 2000 Laser diagnostics of NO reburning in fuel-rich propene flames *Appl. Phys.* B **71** 697–702
[23] Daily J W and Rothe E W 1999 Effect of laser intensity and of lower-state rotational energy transfer upon temperature measurements made with laser-induced fluorescence *Appl. Phys.* B **68** 131
[24] Joklik R G, Horvath J J and Semerjian H G 1991 Temperature measurements in flames using thermally assisted laser-induced fluorescence of Ga *Appl. Opt.* **30** 1497–504
[25] Engström J, Kaminski C F, Aldén M, Josefsson G and Magnusson I 1999 Experimental investigations of flow and temperature fields in an SI engine and comparison with numerical analysis *SAE Paper* 1999-01-3541
[26] Haraguchi H, Smith B, Weeks S, Johnsson D J and Winefordner J D 1977 Measurements of small volume flame temperature y the two-line atomic fluorescence method *Appl. Spectrosc.* **31** 156–63
[27] Engström J, Nygren J, Aldén M and Kaminski C F 2000 Two-line atomic fluorescence as a temperature probe for highly sooting flames *Opt. Lett.* **25** 1469–71
[28] Bonczyk P A 1991 Effects of metal additives on soot precursors and particulates in a $C_2H_4/O_2/N_2$/Ar premixed flame *Fuel* **70** 1403
[29] Kaminski C F, Engström J and Aldén M 1998 Quasi-instantaneous two-dimensional temperature measurements in a spark ignition engine using 2-line atomic fluorescence *Proc. Combust. Inst.* **27** 85–93
[30] Bockhorn H 1994 *Soot Formation in Combustion, Mechanisms and Models (Springer Series in Chemical Physics 59)* (Berlin: Springer) pp 308–15
[31] Mewes B and Seitzman J M 1997 Soot volume fraction and particle size measurement with laser-induced incandescence *Appl. Opt.* **36** 709
[32] Axelsson B, Collin R and Bengtsson P-E 2000 Laser-induced incandescence for soot particle size measurements in premixed flat flames *Appl. Opt.* **39**
[33] Aldén M, Bengtsson P-E and Edner H 1986 Rotational CARS generation through a multiple four-color interaction *Appl. Opt.* **25** 4493–500
[34] Eckbreth A C and Anderson T J 1986 Simultaneous rotational coherent anti-Stokes Raman spectroscopy and coherent Stokes Raman spectroscopy with arbitrary pump-Stokes spectral separation *Opt. Lett.* **11** 496–8
[35] Puri R, Moser M, Santoro R J and Smyth K C 1992 Laser-induced fluorescence measurements of OH concentrations in the oxidation region of laminar hydrocarbon diffusion flames *Proc. Combust. Inst.* **24** 1015
[36] Norton T S, Smyth K C, Miller J H and Smooke M D 1993 Comparison of experimental and computed species concentration and temperature profiles in laminar, two-dimensional methane/air diffusion flames *Combust. Sci. Technol.* **90** 1
[37] Griffiths J F and Barnard J A 1995 *Flame and Combustion* 3rd edn (Oxford: Alden)
[38] Bergmann V, Meier W, Wolff D and Stricker W 1998 Application of spontaneous Raman and Rayleigh scattering and 2D LIF for the characterization of a turbulent $CH_4/H_2/N_2$ jet diffusion flame *Appl. Phys.* B **66** 489–502
[39] Löfström C, Engström J, Richter M, Kaminski C F, Johansson P, Nyholm K, Hult J, Nygren J and Aldén M 2000 Feasibility studies and application of laser/optical diagnostics for characterisation of a practical low-emission gas turbine combustor *ASME Paper* 2000-GT-124.
[40] Shaddix C R and Smyth K C 1996 Laser-induced incandescence measurements of soot production in steady and flickering methane, propane and ethylene diffusion flames *Combust. Flame* **107** 418–52,
[41] Brugman Th M, Stoffels G G M, Dam N, Meerts W L and ter Meulen J J 1997 Imaging and post-processing of laser-induced fluorescence from NO in a diesel engine *Appl. Phys.* B **64** 717
[42] Espey C and Dec J E 1993 Diesel engine combustion studies in a newly designed optical-access engine using high-speed visualization and 2-D laser imaging *SAE Trans.* **102** 703–23
[43] Seitzman J M, Hanson R K, DeBarber P A and Hess C F 1994 Application of quantitative two-line OH planar laser-induced fluorescence for temporally resolved planar thermometry in reacting flows *Appl. Opt.* **33** 4000–12
[44] Dec J E and Keller J O 1986 High speed thermometry using two-line atomic fluorescence *Proc. Combust. Inst.* **21** 1737
[45] International Organisation for Standardization 1995 *Guide to the Expression of Uncertainty in Measurement* 1st edn
[46] Bevington P R and Robinson D K 1992 *Data Reduction and Error Analysis for the Physical Sciences* (Boston: WCB–McGraw-Hill)
[47] 1992 *Handbook of Chemistry and Physics* 63rd edn (Boca Raton, FL: Chemical Rubber Company) pp E243